Journal Pre-proof

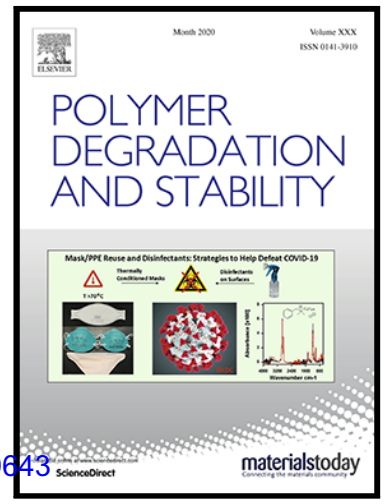

Effect of gamma and neutron irradiation on properties of boron nitride/epoxy resin composites

Limin Jiao , Yi Wang , Zhihao Wu , Hang Shen , Hanqin Weng , Hongbing Chen , Wei Huang , Mozhen Wang , Xuewu Ge , Mingzhang Lin

PII: S0141-3910(21)00163-4
DOI: https://doi.org/10.1016/j.polymdegradstab.2021.109643
Reference: PDST 109643

To appear in: *Polymer Degradation and Stability*

Received date: 9 February 2021
Revised date: 24 May 2021
Accepted date: 31 May 2021

Please cite this article as: Limin Jiao , Yi Wang , Zhihao Wu , Hang Shen , Hanqin Weng , Hongbing Chen , Wei Huang , Mozhen Wang , Xuewu Ge , Mingzhang Lin , Effect of gamma and neutron irradiation on properties of boron nitride/epoxy resin composites, *Polymer Degradation and Stability* (2021), doi: https://doi.org/10.1016/j.polymdegradstab.2021.109643

Highlights

- The mechanical property and T_g of the EP were improved by introducing *h*-BN
- The low contents of *h*-BN were favorable to enhance the radiation resistance of EP
- *h*-BN could weaken oxidative degradation of EP under γ irradiation
- *h*-BN endowed the EP with excellent neutron shielding by absorbing neutrons

Effect of gamma and neutron irradiation on properties of boron nitride/epoxy resin composites

Limin Jiao[a], Yi Wang[a], Zhihao Wu[a], Hang Shen[b], Hanqin Weng[a], Hongbing Chen[b], Wei Huang[b], Mozhen Wang[c], Xuewu Ge[c], Mingzhang Lin[a]*

[a] *Department of Nuclear Science and Engineering, University of Science and Technology of China, Hefei, Anhui 230026, China*

[b] *Institute of Nuclear Physics and Chemistry, China Academy of Engineering Physics, Mianyang, Sichuan 621000, China*

[c] *CAS Key Laboratory of Soft Matter Chemistry, Department of Polymer Science and Engineering, University of Science and Technology of China, Hefei, Anhui 230026, China*

* To whom correspondence should be addressed. E-mail: gelin@ustc.edu.cn (M.Z. Lin).

Abstract

Improving the radiation resistance of epoxy resin (EP) is pivotal for the reliability of equipment and the safety of facilities in the nuclear industry. Hexagonal boron nitride (*h*-BN) is attractive in the preparation of radiation-resistant materials due to its good radiation stability and neutron shielding capability. In this work, *h*-BN/EP composites with enhanced radiation resistance were fabricated by solution blending. The tensile strength and thermal properties of the composites after γ-ray and neutron irradiation were investigated. The results showed that the addition of *h*-BN improved the mechanical property and the glassy transition temperature of the resin. The presence of low-level *h*-BN was favorable to enhance the radiation resistance of EP. As for composites with the 0.05% mass percentage of *h*-BN, the absorbed dose required to decrease relative tensile strength by 50% was about 300 kGy, which was higher than that of neat EP. The intrinsic

mechanism of radiation resistance was attributed to the oxygen barrier effect as investigated by XPS and EPR. Then, benefiting from the absorbing neutrons capability of boron atoms, an addition of 0.55% *h*-BN to the EP resin could reduce the neutron transmittance of the resin by 5.6%. This study demonstrates that the blending with *h*-BN can increase the radiation-resistant property of EP resin, meanwhile augmenting the neutron shielding ability.

Keywords: epoxy resin, hexagonal boron nitride, γ-ray irradiation, neutron shielding, stability

1. Introduction

Polymer materials are widely used in nuclear power plants and other nuclear facilities owing to their low density, high strength and specific modulus. However, they will inevitably be affected by ionizing radiation, such as γ-ray, electron beam and neutron beam [1, 2]. The ionizing radiation can cause atomic displacement and electronic excitation of materials, which severely worsen the critical properties of structural material [3, 4]. Being high-performance thermosetting resin, epoxy resin (EP) has been widely used as encapsulation materials for electronic devices, embedding materials for low and intermediate level radioactive waste and organic coatings for the containment, thanks to its excellent electrical and mechanical property [5]. Yet the high-dose irradiation generally degrades the properties of EP and even causes serious engineering accidents [6]. Therefore, the development of radiation-resistant EP possesses crucial theoretical significance and engineering value for enhancing the reliability of equipment and ensuring the safety of nuclear facilities.

The radiation effect and radiation-damage mechanism of EP have been extensively studied in the world over the past 50 years [7, 8]. It is confirmed that the incorporation of some special inorganic or organic radiation-resistant substances into EP can markedly raise the radiation

stability, such as lead, tungsten, and aromatic compounds [9, 10]. Unfortunately, the poor compatibility between the filler and EP leads to the substantially decreased strength of the composite with the increase of the additives. In addition, the radiation resistance of EP can be improved by adding another polymer material with good compatibility with the EP and containing radiation resistant groups, or by directly modifying the EP and introducing aromatic groups [11]. Although these techniques enhanced the radiation stability of materials, they caused somewhat decrease of the mechanical properties of composites before irradiation. It is desirable to prepare EP composites with excellent mechanical properties and radiation resistance.

Two-dimensional materials have been proved to be fascinating fillers for the construction of functional composites with numerous applications [12]. As a structural analogue of graphite, hexagonal boron nitride (*h*-BN) shows the excellent mechanical property, thermal stability, and neutron shielding [13-15], which has been regarded as a promising candidate to fabricate EP composites with integrated performance. Introduction of hydroxylated *h*-BN can enhance the thermal stability, flame retardancy and smoke suppression of EP. The char yield and the temperature at 50 *wt*% mass loss of composites increased, and the peak heat release rate, total heat release, and release of smoke and toxic gases decreased [16]. The EP nanocomposites with tannic acid-modified *h*-BN nanosheets showed the excellent anticorrosion effect on the metal substrates and good anticorrosion stability after being immersed in 3.5 *wt*% NaCl aqueous solution for 120 h [17]. To the best of our knowledge, most of the research focusing on the thermal and corrosion properties of *h*-BN/EP. There are very few reports on its radiation protection performance. Saiyad *et al*. dispersed *h*-BN uniformly into EP by gravity casting method, resulting in the neutron linear absorption coefficient of *h*-BN/EP was 1.16 times as high as lead/EP [18]. The neutron shielding

performance of *h*-BN/EP has been documented, yet no information is available on the radiation stability of *h*-BN/EP exposure to γ-rays.

In this study, di-glycidyl 4,5-epoxycyclohexane-1,2-dicarboxylate (TDE-85) with high reactivity and excellent electrical insulation performance was selected as a monomer of EP. *h*-BN/EP composites were prepared by solution blending. The tensile strength and thermal stability confirmed the radiation resistance enhancement in the case of the addition of *h*-BN. X-Ray photoelectron spectroscopic (XPS) and Electronic paramagnetic resonance (EPR) analysis were employed to investigate the mechanism of enhanced radiation resistance. The small angle neutron scattering (SANS) spectrometer was employed to investigate the neutron shielding capability, further understanding the effect of *h*-BN.

2 Experimental section

2.1 Materials

The *h*-BN powder (~ 325 mesh, 99.5%) was obtained from Shanghai Alfa Aesar Co. Ltd. TDE-85 was brought from Hubei Xinkang Pharmaceutical Chemical Co. Ltd. Methyl hexahydrophthalic anhydride (MHHPA, 98%) was purchased from Shanghai Macklin Biochemical Co. Ltd. The molecular structure of TDE-85 and MHHPA was shown in Scheme S1. The 2,4,6-tris (dimethylaminomethyl) phenol (DMP-30, 95%) was obtained from Shanghai Aladdin Bio-Chem Technology Co. Ltd. High purity nitrogen (≥ 99.999%) was supplied by Nanjing Shangyuan Industrial Gas Factory. All of the above materials were used directly without further purification.

2.2 Composites preparation

The *h*-BN/EP composites were prepared via solution blending method as the synthesis route in

Fig. 1. In a typical procedure, 22.09 g of TDE-85 was put into a 100 mL beaker and then degassed at 60°C for 30 min in a vacuum oven. After adding 15 mL of MHHPA, 220 μL of DMP-30 and a given amount of *h*-BN to the beaker successively, the mixed solution was stirred for 12 h and degassed for 30 min again. Then, the mixture was poured into the tailored stainless steel molds. The samples were solidified according to the predetermined heating program of 80, 130 and 180°C for 2 h, respectively, and finally cooled down to room temperature. The curing temperature was determined by non-isothermal DSC measurements (Fig. S1 and Table S1). The final products were termed as *h*-BN/EP-*x*, where the *x* (0.02%,0.05%, 0.15%, 0.25%, 0.55%) denoted the mass percent of *h*-BN to EP.

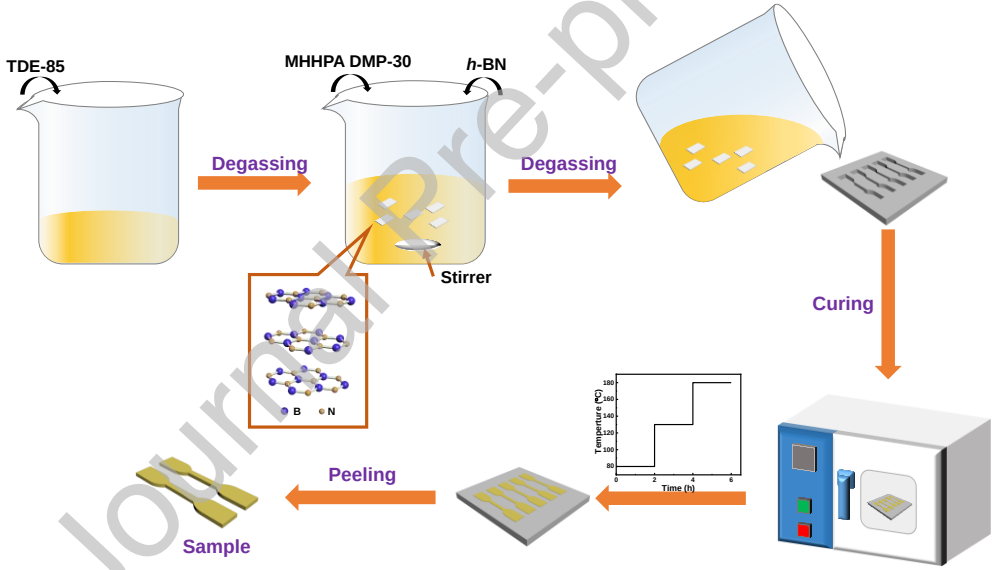

Fig 1. Schematic diagram of the preparation processes of *h*-BN/EP composites.

2.3 Irradiation experiments

The *h*-BN/EP samples were placed into glass bottles. Some bottles were unsealed, while the others were sealed after purging with nitrogen for 15 min to remove oxygen. The samples were exposed to ^{60}Co γ-ray radiation field (20 kCi, located in the University of Science and Technology of China) with an absorbed dose rate of 65 Gy min^{-1} at ambient temperature. The absorbed dose

rate was calibrated by alanine/EPR standard dosimeter. Neutron radiation was carried out in the China Fast Burst Reactor II (CFBR II) at the Institute of Nuclear Physics and Chemistry, China Academy of Engineering Physics, at a neutron fluence rate of ~10^9 cm^{-2} s^{-1} in steady power mode.

2.4 Characterization

The tensile strength of the samples was determined at room temperature according to the national standard method of China for plastic tensile properties (No. GB-T1040.3-2006). The fracture stress test was implemented on an Instron electronic dynamic and static fatigue tester (E3000K8953) with the tensile speed of 1 mm min^{-1}. Each sample was tested five times and the average was used as the final result. The UV–vis diffuse reflectance spectra were collected on a SOLID3700 spectrophotometer. The scanning electron microscope (SEM, SU8220, 5.0 kV) was used to observe the fracture surface morphologies of the samples. The thermal stability was assessed over a thermogravimetric analyzer (SDTQ600) under nitrogen atmosphere at a heating rate of 10°C min^{-1}. The glass transition temperature (T_g) was measured on a differential scanning calorimeter (DSC Q2000) under nitrogen atmosphere. The sample was heated from 30 to 250°C at a rate of 10°C min^{-1} and cycled three times. Attenuated total reflectance Fourier-transform infrared spectra (ATR-FTIR) were obtained using a Bruker Tensor 27 spectrometer in the wavenumber range from 4000 to 400 cm^{-1}. X-Ray photoelectron spectroscopic (XPS) measurements were realized on a Thermo ESCALAB 250XI with monochromatic Al Kα radiation (hv = 1486.6 eV, 200 W). And the major C *1s* peak at 284.8 eV was selected as the reference for binding energy. Electronic paramagnetic resonance (EPR) test was carried out on a JEOL JES-FA200 spectrometer with the frequency of 9.080 GHz and the magnetic field scanning range

of 299.5 ~ 349.5 mT. The signal intensity was normalized with sample mass to compensate for the mass-derived error. Neutron shielding characterization was carried out on SANS spectrometer Suanni at the China Mianyang Research Reactor (CMRR) in Mianyang [19]. The neutron wavelength was λ = 0.53 nm with a spread of $\Delta\lambda/\lambda$ = 10% and beam diameter of 8 mm. The sample-to-detector distance was chosen as 10 m. The transmission was measured as the ratio of the direct beam intensity with and without the sample.

3 Results and discussion

3.1 Mechanical and thermal properties of h-BN/EP composites

The photograph of neat EP and *h*-BN/EP (Fig. 2a) revealed that the transparency of strips decreased as the *h*-BN content increased. The transmittance of the samples in the wavelength range from 300 to 800 nm (Fig. S2) decreased with increasing *h*-BN content, confirming well the same trend of coloration. This photograph indicated that *h*-BN had been successfully added to the EP. The tensile properties of the neat EP and *h*-BN/EP composites were measured as shown in Fig. 2b. With increasing *h*-BN content, the tensile strength increased firstly and then decreased. The maximal tensile strength was 71.1 MPa with the 0.05% of *h*-BN filler, which was higher than that of neat EP. It has been reported that the loading *h*-BN could transfer stress and produce micro-cracks in the composites, the micro-cracks absorbed energy and prevented the cracks from developing into destructive cracks [20]. At high *h*-BN content, the filler agglomerates might be regarded as the stress concentration points, evolving gradually into macroscopic stress crack, which should be responsible for the decrease of tensile strength [21].

SEM images of the fracture surface of EP and *h*-BN/EP after tensile testing were presented in Figs. 2c–e. The smooth and featureless surface of neat EP could be observed in Fig. 2c, which

possessed many river-like stripes and provided weak locations at the plastic deformation under external loads. The fracture surfaces of *h*-BN/EP-0.05% became rougher than the neat EP. The main reason was that the fillers embedded in the epoxy matrix limited the mobility capacity of the polymer molecule chain segments and induced the micro-cracks to absorb deformation energy under an external force, resulting in fracture energy consumption and the enhanced tensile strength of the composites [22]. However, *h*-BN/EP-0.55% represented lower surface roughness than *h*-BN/EP-0.05%, which was connected with serious aggregation and poor dispersion of the excessive fillers in the composites.

The incorporation of fillers into a polymer matrix can bring about changes in the thermal characteristics of the resulting composites. One benchmark used to compare the thermal behavior of composites is the T_g. DSC measurements were carried out to analyze the effect of different *h*-BN contents on the T_g. It can be seen from Fig. 2f that the T_g of neat EP was 111.7°C. After adding *h*-BN, the T_g displayed an increasing trend with filler concentration. The increment was attributed to the interaction between the matrix and *h*-BN, which hindered the mobility of matrix chains near the *h*-BN [23].

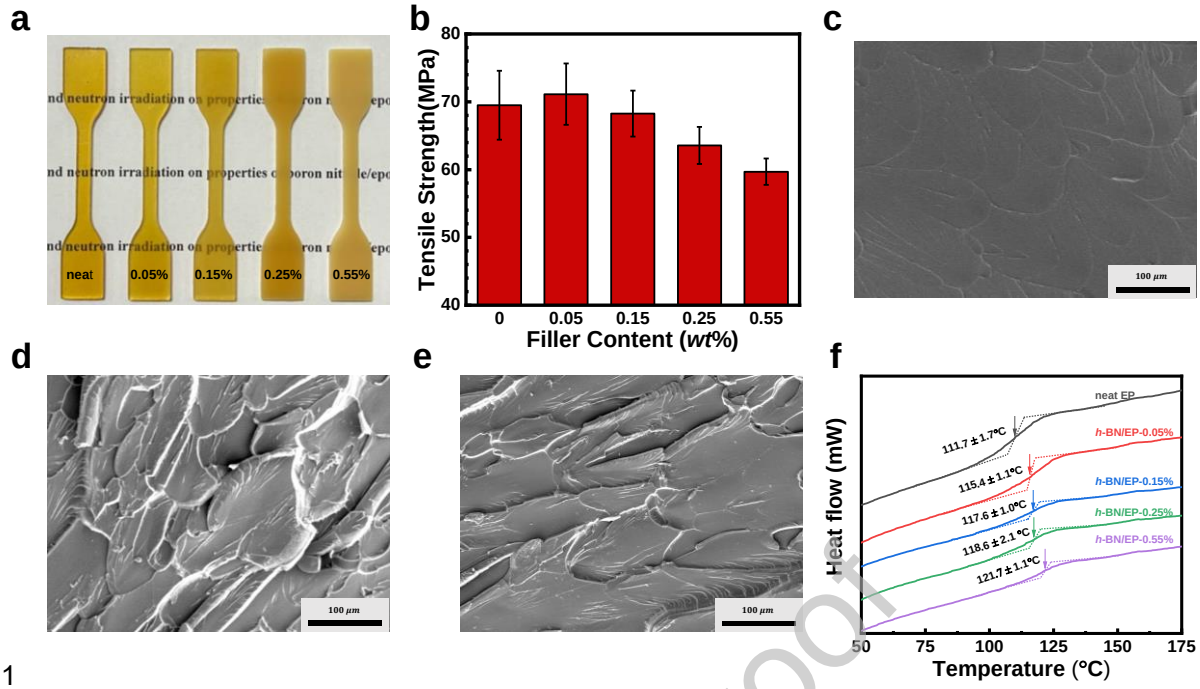

Fig. 2. Optical photograph (a), tensile strength (b) of neat EP and *h*-BN/EP; SEM images of the fracture surface of neat EP (c), *h*-BN/EP-0.05% (d) and *h*-BN/EP-0.55% (e); DSC curves (f) of neat EP and *h*-BN/EP.

3.2 The γ-radiation stability of EP and h-BN/EP

The previous literature proved that radiation can cause polymers to crosslink or chain scission, and their radiation stability can be evaluated by comparing the mechanical and thermal properties before and after irradiation [24]. As shown in Fig. 3a, the color of EP changed from light yellow to brown as the absorbed dose increased. The UV–vis absorption spectra of the irradiated EP (Fig. S3) showed a progressive redshift as the absorbed dose increased, which was consistent with the increase of color degree. Variation of strips color might be attributed to the formation of conjugated unsaturated bonds. This chemical system produced color centers that absorbed at a specific wavelength [25] The variation of the tensile strength of neat EP with absorbed irradiation dose was shown in Fig. 3b. The tensile strength exhibited similar behavior regardless of the irradiation atmosphere, raised first and then dropped with the increase of dose. In the case of low

absorbed dose (≤ 282 kGy), there was little change in tensile strength of samples whatever the atmospheres were air or nitrogen, demonstrating that the effect of oxygen was limited by the slow oxygen diffusion and short diffusion depth at the surface. In particular, when absorbed dose was 188 kGy, the tensile strength was 79.87 MPa, that is, an increase of 15%. Moreover, it could be seen that the strain softening occurred in low absorbed dose from the stress-strain curves in Figs. 3c and 3d. All results indicated that radiation-induced crosslinking played a dominant role in the case of low absorbed dose. The free radicals generated from γ-ray irradiation could crosslink the uncured epoxy bond, resulting in the enhanced tensile strength. However, under the higher absorbed dose, the mechanical property greatly deteriorated. When absorbed dose was up to 1880 kGy, the tensile strength of samples exposed to air and nitrogen was reduced by 70% and 58%, respectively. Obviously, at a high absorbed dose, radiation-induced chain scission was the primary process, and the process was inhibited in the anaerobic atmosphere.

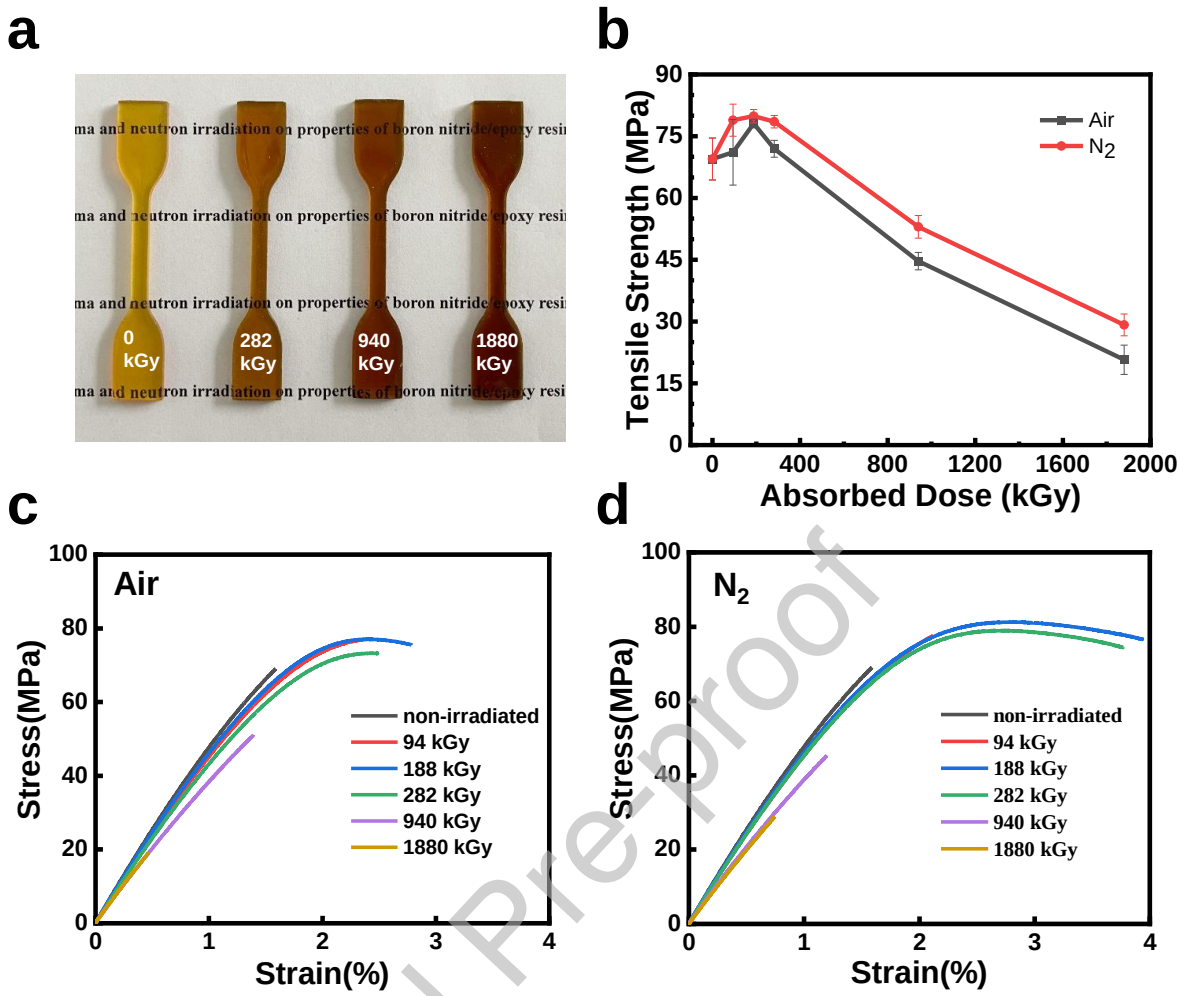

Fig. 3. Optical photograph (a), tensile strength (b), and stress-strain curves under air atmosphere (c) and nitrogen atmosphere (d) of EP before and after irradiation.

The γ-ray radiation resistance of *h*-BN/EP was studied over the diverse filler-content composites. The radiation resistance of the samples was evaluated at 50% tensile strength from a linear extrapolation between the two last points [26], where the relative tensile strength of samples was calculated by the following equation:

$$Relative\ tensile\ strength\ (\%) = \frac{tensile\ strength\ of\ \ samples\ after\ irradiation}{tensile\ strength\ of\ samples\ before\ irradiation} \quad (1)$$

From the relation of relative tensile strength with absorbed dose in Figs. 4a and 4b, the variation tendency of tensile strength of *h*-BN/EP composites was similar with that of neat EP after γ-ray

irradiation. The strength of composites had been increased gradually until the absorbed dose reached 282 kGy, then decreased significantly as the absorbed dose further increased. When the tensile strength was reduced by 50%, the absorbed dose of *h*-BN/EP-0.05% was higher than other samples, especially 300 kGy higher than that of neat EP. The *h*-BN/EP-0.05% gave much higher radiation resistance than neat EP. However, *h*-BN/EP-0.55% presented poor performance because the strength of composites was strongly affected by particle/matrix adhesion [27]. Thus, adding low-content *h*-BN was conducive to improving the radiation resistance of EP. Besides, the tensile strength of all irradiated samples decreased more slowly under nitrogen atmosphere compared with that in ambient condition, suggesting that oxygen accelerates the radiation degradation of *h*-BN/EP.

It is well-known that thermal stability of epoxy resins is related closely to their cross-linking density. The resin with higher cross-linking density usually has better thermal stability [28]. Nevertheless, the radiation-induced decomposition could destruct the cross-linked structure and even the skeleton of epoxy resin, resulting in the declined thermal property of the resins [29]. DSC was further hired to measure the T_g of neat EP and *h*-BN/EP-0.05% after irradiation. From Fig. 4c, under air atmosphere, the T_g of both EP and *h*-BN/EP-0.05% samples decreased by about 30℃ after γ-ray irradiation with an absorbed dose of 1880 kGy, while it decreased only about 25℃ under nitrogen. This reflected the increase of chain mobility resulting from chain scissions. From the TGA curves in Fig. 4d, the initial decomposition temperature of irradiated samples was lower than that of non-irradiated samples. The results of DSC and TGA indicated that γ-ray irradiation lowered the thermal stability of all samples with or without 0.05% *h*-BN.

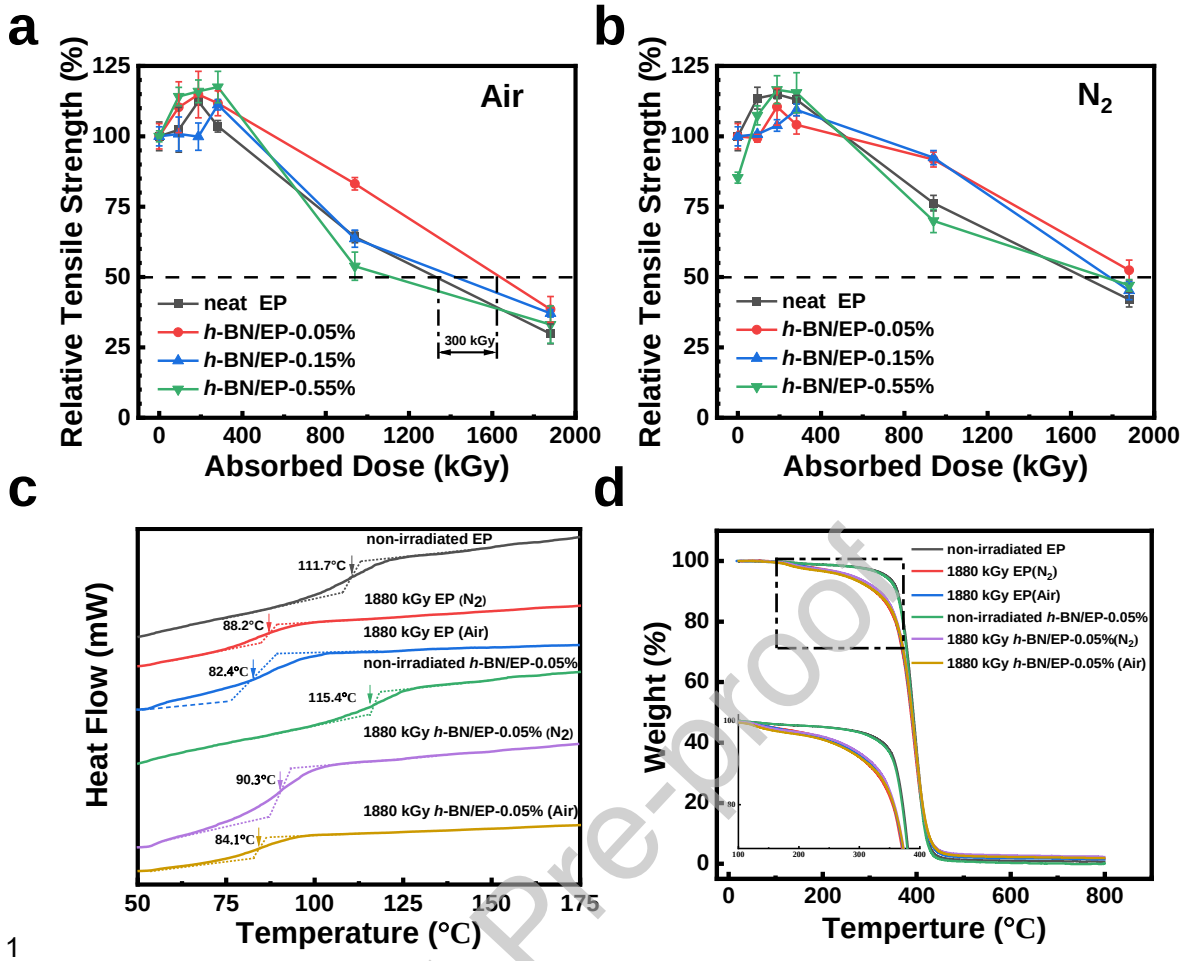

Fig. 4. The tensile strength of neat EP and *h*-BN/EP-*x* (*x* = 0.05, 0.15, and 0.55%) composites before and after irradiation: under air atmosphere (a) and nitrogen atmosphere (b). DSC curves (c) and TGA curves (d) of EP and h-BN/EP-0.05% composites with 1880 kGy of absorbed dose.

3.3 γ-Ray irradiation damage mechanism of h-BN/EP

In order to understand the change of interior chemical composition by γ-ray irradiation, the samples were cryogenically fractured in liquid nitrogen, and the chemical composition of the fracture surface was measured by XPS. Fig. 5 showed the high-resolution C *1s* XPS spectra for the interior of samples before and after γ-radiation of 1880 kGy. Obviously, the C *1s* signal could be deconvolved into three peaks located at 284.8, 286.4, and 288.9 eV, assignable to C–H/C–C, C–O, and C=O, respectively [30]. The oxidation degree (OD) of sample was defined as the sum of the

area ratio of C–O and C=O. The equation was shown below:

$$OD(\%) = \text{area ratio of C–O} + \text{area ratio of C=O} \quad (2)$$

As shown in Table 1, the OD of neat EP was raised to 41.94% and 42.07% after irradiation in air and nitrogen respectively. The same increase tendency regardless of the atmosphere might attribute to the effect of dissolved oxygen. Park *et al*. found that the dissolved oxygen which may not be completely removed even under the continuous vacuum treatment may cause oxidation reactions [31]. The C–H/C–C bonds were broken by γ irradiation, which would undergo oxidation reaction with dissolved oxygen and eventually resulted in oxidative degradation. Similar results were also observed in *h*-BN/EP-0.05%, but the increase was less than neat EP. This indicated that filling *h*-BN into EP was beneficial to hinder the oxidative degradation of EP under γ irradiation.

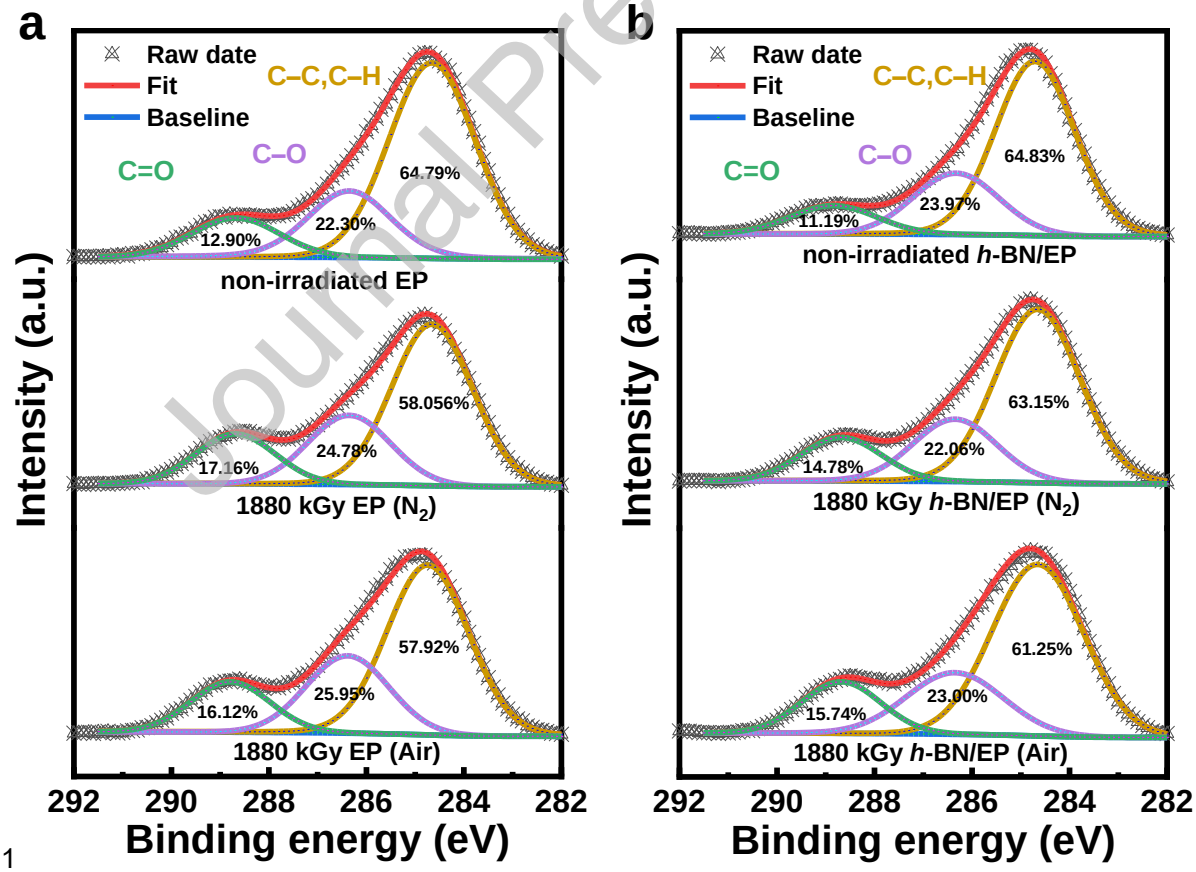

Fig. 5. High-resolution C 1s XPS spectra for the interior of samples before and after irradiation: neat EP (a); *h*-BN/EP-0.05% (b).

Table 1. The oxidation degree (OD) of the interior of samples before and after irradiation.

Samples	Oxidation degree (%)
non-irradiated EP	35.20
1880 kGy EP (N_2)	41.94
1880 kGy EP (Air)	42.07
non-irradiated *h*-BN/EP	35.17
1880 kGy *h*-BN/EP (N_2)	36.85
1880 kGy *h*-BN/EP (Air)	38.75

Room-temperature EPR measurement was performed to detect the active radicals of EP before and after γ-ray irradiation. From Fig. 6a, the signal peaks were not detected for the non-irradiated EP, while the asymmetric wide signal peaks were clearly observed after irradiation, suggesting the generation of radiation-induced radicals. According to the previous reports, this signal should be assigned to alkoxy or peroxy radicals [32, 33]. It could be seen that when the sample was exposed to γ-ray with the absorbed dose of 94 kGy, the signal of free radicals appeared. These free radicals might be generated by the rupture of some weak bonds. The intensity of free radicals' signals went up with the absorbed dose because more bonds were broken.

As for *h*-BN/EP composites, the radical concentration varied under different atmospheres

(Fig. 6b and 6c). In the air, the radical amount of *h*-BN/EP was fewer than that of neat EP, while was basically unchanged under nitrogen. As shown in Fig. 6b, a small content of *h*-BN (0.02%, 0.05%) could significantly inhibit radical production, resulting in the enhanced oxidative stability of composite compared to neat epoxy. Combining with XPS spectra of the samples irradiated in air, the area ratios for C–O and C=O of *h*-BN/EP-0.05% were fewer than neat EP, thereby we could speculate that a relatively small amount of *h*-BN (0.02%, 0.05%) had a better dispersibility and prevents oxidation of EP [34]. Yet the radical concentration ascended evidently at the filling level of 0.15% and 0.55%, which indicated that further increasing filling level was less effective. This phenomenon could be explained that the addition of excessive *h*-BN might cause agglomeration.

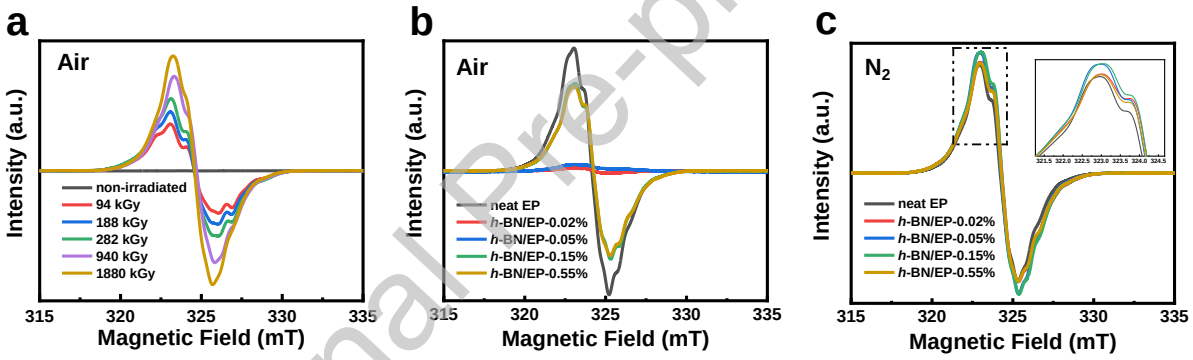

Fig. 6. EPR curves (a) of neat EP at different absorbed doses. EPR curves of EP with different *h*-BN content after irradiation at 1880 kGy in air (b) and in nitrogen (c).

3.4 The neutron radiation stability of EP and h-BN/EP

Neutrons and γ rays are the main types of radiation in nuclear facilities, so the neutron radiation stability and neutron shielding properties of EP and *h*-BN/EP must also have to be considered. The photograph of samples showed that there was no obvious change in the samples before and after neutron irradiation (Fig. 7a). This could be due to the fact that the neutron fluence is not high enough to generate visible coloration in the experiments. As shown in Fig. 7b, the tensile strength

of all the samples showed little change, indicating that the resin matrix was not sensitive to neutron irradiation at the neutron fluence of 10^{14} n cm^{-2}. In addition, as illustrated in Fig. S5, the initial decomposition temperature of the samples did not change significantly, suggesting the fine thermal property of *h*-BN/EP after neutron irradiation. In Fig. 7c, there is a clear trend of decreasing the neutron transmittance with the increase of *h*-BN content. The neutron transmittance of *h*-BN/EP-0.55% was 36.9%, which lowered than that of EP (42.5%), indicating the enhanced neutron shielding performance. This should be attributed to the fact that the boron atoms in *h*-BN absorb neutrons [35].

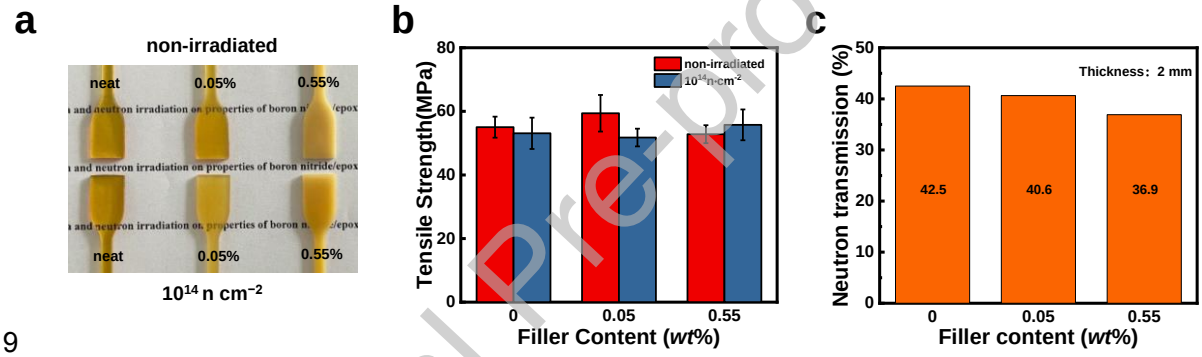

Fig. 7. Optical photograph (a) and tensile strength (b) of EP and *h*-BN/EP-*x* (*x* = 0.05% and 0.55%) irradiated at the neutron fluence of 10^{14} n cm^{-2}, neutron shielding property (c) of EP and *h*-BN/EP-*x* (*x* = 0.05% and 0.55%).

4 Conclusion

In this study, *h*-BN/EP composites were synthesized, and their radiation resistance towards γ-ray and neutron beam was evaluated. It has been shown that the addition of a small amount of *h*-BN (0.05%) can enhance the mechanical property. After γ-ray irradiation, the tensile strength of composites increased first and then decreased with the increase of absorbed dose. Furthermore, radiation degradation of composites was inhibited with the addition of *h*-BN. The absorbed dose of *h*-BN/EP-0.05% was about 300 kGy higher than that of neat EP when the relative tensile

strength is reduced by half. Combined with the results of XPS and EPR, *h*-BN could weaken oxidative degradation of EP under γ irradiation. The mobility of the EP molecule chains was reduced after introducing *h*-BN, and more free radicals were trapped in the polymer chain, restraining the further reaction. In the case of neutron irradiation, *h*-BN can improve neutron shielding performance and absorb energy to reduce radiation damage. This work demonstrates that *h*-BN is an advantageous candidate in improving the radiation resistance and neutron shielding of the EP, also probably available to enhance the radiation resistance of other polymer materials. Furthermore, based on this work, the influence of *h*-BN size and interface effect on epoxy resin will be further studied.

Acknowledgments

This work was supported by the Science Challenging Project (TZ2018004) and the National Natural Science Foundation of China (No. 11775214 and 51803205).

References

[1] S.G. Burnay, An overview of polymer ageing studies in the nuclear power industry, Nucl. Instrum. Meth. B. 185 (2001) 4-7.

[2] V. Placek, T. Kohout, V. Hnat, B. Bartonicek, Assessment of the EPDM seal lifetime in nuclear power plants, Polym. Test. 28(2) (2009) 209-214.

[3] M. Celina, E. Linde, D. Brunson, A. Quintana, N. Giron, Overview of accelerated aging and polymer degradation kinetics for combined radiation-thermal environments, Polym. Degrad. Stabil. 166 (2019) 353-378.

[4] S.A. Thibeault, J.H. Kang, G. Sauti, C. Park, C.C. Fay, G.C. King, Nanomaterials for radiation shielding, Mrs. Bull. 40(10) (2015) 836-841.

[5] R. Li, Y. Gu, Z. Yang, M. Li, S. Wang, Z. Zhang, Effect of γ irradiation on the properties of basalt fiber reinforced epoxy resin matrix composite, J. Nucl. Mater. 466 (2015) 100-107.

[6] F. Djouani, Y. Zahra, B. Fayolle, M. Kuntz, J. Verdu, Degradation of epoxy coatings under gamma irradiation, Radiat. Phys. Chem. 82 (2013) 54-62.

[7] K.P. Chen, X.L. Zhao, F.S. Zhang, X.L. Wu, W. Huang, W. Liu, X.L. Wang, Influence of gamma irradiation on the molecular dynamics and mechanical properties of epoxy resin, Polym. Degrad. Stabil. 168 (2019) 108940.

[8] F. Diao, Y. Zhang, Y. Liu, J. Fang, W. Luan, γ-Ray irradiation stability and damage mechanism of glycidyl amine epoxy resin, Nucl. Instrum. Meth. B. 383 (2016) 227-233.

[9] A. Canel, H. Korkut, T. Korkut, Improving neutron and gamma flexible shielding by adding medium-heavy metal powder to epoxy based composite materials, Radiat. Phys. Chem. 158 (2019) 13-16.

[10] C.G. Delides, The protective effect of phenyl group on the crosslinking of iradiated dimethyldiphenylsiloxane, Radiat. Phys. Chem. 16(5) (1980) 345-352.

[11] J. Schutz, R. Reed, D. Evans, Radiation resistant epoxy for resin transfer molding fabrication of cryogenic electrical insulation, Adv. Cryog. Eng. 46 (2000) 197-204.

[12] K.S. Novoselov, D. Jiang, F. Schedin, T.J. Booth, V.V. Khotkevich, S.V. Morozov, A.K. Geim, Two-dimensional atomic crystals, P. Natl. Acad. Sci. USA. 102(30) (2005) 10451-10453.

[13] L. Boldrin, F. Scarpa, R. Chowdhury, S. Adhikari, Effective mechanical properties of hexagonal boron nitride nanosheets, Nanotechnology 22(50) (2011) 505702.

[14] W.L. Song, P. Wang, L. Cao, A. Anderson, M.J. Meziani, A.J. Farr, Y.P. Sun, Polymer/boron nitride nanocomposite materials for superior thermal transport performance, Angew. Chem. Int. Edit. 51(26)

(2012) 6498-6501.

[15] S.G. Irim, A.A. Wis, M.A. Keskin, O. Baykara, G. Ozkoc, A. Avci, M. Dogru, M. Karakoc, Physical, mechanical and neutron shielding properties of *h*-BN/Gd_2O_3/HDPE ternary nanocomposites, Radiat. Phys. Chem. 144 (2018) 434-443.

[16] B. Yu, W. Xing, W. Guo, S. Qiu, X. Wang, S. Lo, Y. Hu, Thermal exfoliation of hexagonal boron nitride for effective enhancements on thermal stability, flame retardancy and smoke suppression of epoxy resin nanocomposites via sol-gel process, J. Mater. Chem. A 4(19) (2016) 7330-7340.

[17] D. Pan, X. Zhang, G. Yang, Y. Shang, F. Su, Q. Hu, R.R. Patil, H. Liu, C. Liu, Z. Guo, Thermally conductive anticorrosive epoxy nanocomposites with tannic acid-modified boron nitride nanosheets, Ind. Eng. Chem. Res. 59(46) (2020) 20371-20381.

[18] M. Saiyad, N.M. Devashrayee, R.K. Mevada, Study the effect of dispersion of filler in polymer composite for radiation shielding, Polym. Composite. 35(7) (2014) 1263-1266.

[19] L. Chen, L.W. Sun, Y. Wang, Y.L. Wang, L. Zou, G.Y. Yan, J. Chen, Q. Tian, M. Peng, J. Gong, B. Chen, G.G. Sun, D. Liu, Small-angle neutron scattering spectrometer suanni equipped with ultra-thin biconcave focusing lenses, J. Appl. Crystallogr. 49 (2016) 1388-1393.

[20] H. Akhina, M.R.G. Nair, N. Kalarikkal, K.P. Pramoda, T.H. Ru, L. Kailas, S. Thomas, Plasticized PVC graphene nanocomposites: morphology, mechanical, and dynamic mechanical properties, Polym. Eng. Sci. 58 (2018) E104-E113.

[21] S. Zhao, L.S. Schadler, R. Duncan, H. Hillborg, T. Auletta, Mechanisms leading to improved mechanical performance in nanoscale alumina filled epoxy, Compos. Sci. Technol. 68(14) (2008) 2965-2975.

[22] M. Derradji, N. Ramdani, T. Zhang, J. Wang, T. Feng, H. Wang, W. Liu, Mechanical and thermal

properties of phthalonitrile resin reinforced with silicon carbide particles, Mater. Design. 71 (2015) 48-55.

[23] J. Joy, E. George, S. Thomas, S. Anas, Effect of filler loading on polymer chain confinement and thermomechanical properties of epoxy/boron nitride (*h*-BN) nanocomposites, New J. Chem. 44(11) (2020) 4494-4503.

[24] T. Zaharescu, I. Plesa, S. Jipa, Kinetic effects of silica nanoparticles on thermal and radiation stability of polyolefins, Polym. Bull. 70(11) (2013) 2981-2994.

[25] R. Clough, G. Malone, K. Gillen, J. Wallace, M. Sinclair, Discoloration and subsequent recovery of optical polymers exposed to ionizing radiation, Polym. Degrad. Stabil. 49(2) (1995) 305-313.

[26] G. Burillo, M.F. Beristain, E. Sanchez, T. Ogawa, Effects of aromatic diacetylenes on polyurethane degradation by gamma irradiation, Polym. Degrad. Stabil. 98(10) (2013) 1988-1992.

[27] S. Fu, X. Feng, B. Lauke, Y. Mai, Effects of particle size, particle/matrix interface adhesion and particle loading on mechanical properties of particulate–polymer composites, Compos. B. Eng. 39(6) (2008) 933-961.

[28] F. Jeyranpour, G. Alahyarizadeh, B. Arab, Comparative investigation of thermal and mechanical properties of cross-linked epoxy polymers with different curing agents by molecular dynamics simulation, J. Mol. Graph. Model. 62 (2015) 157-164.

[29] J. Davenas, I. Stevenson, N. Celette, S. Cambon, J.L. Gardette, A. Rivaton, L. Vignoud, Stability of polymers under ionising radiation: The many faces of radiation interactions with polymers, Nucl. Instrum. Meth. B. 191 (2002) 653-661.

[30] G. Beamson, High resolution XPS of organic polymers, The Scienta ESCA 300 Database (1992).

[31] J. Park, K. Seo, R. Fornes, R. Gilbert, Effects of ionizing radiation on epoxys, graphite fiber and

their composites, Plast. Rubber. Process.Appl. 10(4) (1988) 203-209.

[32] K.S. Seo, R.E. Fornes, R.D. Gilbert, J.D. Memory, Effects of ionizing radiation on epoxy, graphite fiber, and epoxy/graphite fiber composites. Part II: radical types and radical decay behavior, J. Polym. Sci. Pol. Phys. 26(3) (1988) 533-544.

[33] W. Xia, H.R. Xue, J.W. Wang, T. Wang, L. Song, H. Guo, X.L. Fan, H. Gong, J.P. He, Functionlized graphene serving as free radical scavenger and corrosion protection in gamma-irradiated epoxy composites, Carbon 101 (2016) 315-323.

[34] Z.B. Niu, L. Zhuan, X. Peng, J.W. Li, Z.C. Li, O.Y. Xi, L. Yang, Influence of *h*-BN as additive on microstructure and oxidation mechanism of C/C-SiC composite, J. Eur. Ceram. Soc. 39(15) (2019) 4634-4644.

[35] A. Morioka, S. Sakurai, K. Okuno, S. Sato, Y. Verzirov, A. Kaminaga, T. Nishitani, H. Tamai, Y. Kudo, S. Yoshida, Development of 300°C heat resistant boron-loaded resin for neutron shielding, J. Nucl. Mater. 367 (2007) 1085-1089.

Limin Jiao: Data curation, Validation, Conceptualization, Writing - original draft. **Yi Wang:** Investigation, Formal analysis. **Zhihao Wu**: Conceptualization, Writing - review & editing. **Hang Shen:** Formal analysis. **Hanqin Weng**: Writing - review & editing Funding acquisition. **Hongbing Chen:** Funding acquisition, Resources. **Wei Huang:** Funding acquisition, Resources. **Mozhen Wang:** Writing - review & editing. **Xuewu Ge:** Writing - review & editing. **Mingzhang Lin:** Supervision, Project administration, Funding acquisition.

Declaration of Competing Interest

We declare that we have no financial and personal relationships with other people or organizations that can inappropriately influence our work, there is no professional or other personal interest of any nature or kind in any product, service and/or company that could be construed as influencing the position presented in, or the review of, the manuscript entitled.

Graphical Abstract